European Radiology (2023) 33:4700–4712
https://doi.org/10.1007/s00330-023-09618-9

European Radiology
ESR EUROPEAN SOCIETY OF RADIOLOGY

CHEST

Pulmonary circulation abnormalities in post-acute COVID-19 syndrome: dual-energy CT angiographic findings in 79 patients

Islam Mohamed[1] · Virginie de Broucker[2] · Alain Duhamel[3] · Jessica Giordano[1] · Alice Ego[1] · Nicolas Fonne[1] · Cécile Chenivesse[4] · Jacques Remy[1] · Martine Remy-Jardin[1,5]

Received: 8 December 2022 / Revised: 26 February 2023 / Accepted: 6 March 2023 / Published online: 25 April 2023

Abstract

Objectives To evaluate the frequency and pattern of pulmonary vascular abnormalities in the year following COVID-19.

Methods The study population included 79 patients remaining symptomatic more than 6 months after hospitalization for SARS-CoV-2 pneumonia who had been evaluated with dual-energy CT angiography.

Results Morphologic images showed CT features of (a) acute (2/79; 2.5%) and focal chronic (4/79; 5%) PE; and (b) residual post COVID-19 lung infiltration (67/79; 85%). Lung perfusion was abnormal in 69 patients (87.4%). Perfusion abnormalities included (a) perfusion defects of 3 types: patchy defects ($n=60$; 76%); areas of non-systematized hypoperfusion ($n=27$; 34.2%); and/or PE-type defects ($n=14$; 17.7%) seen with (2/14) and without (12/14) endoluminal filling defects; and (b) areas of increased perfusion in 59 patients (74.9%), superimposed on ground-glass opacities (58/59) and vascular tree-in-bud (5/59). PFTs were available in 10 patients with normal perfusion and in 55 patients with abnormal perfusion. The mean values of functional variables did not differ between the two subgroups with a trend toward lower DLCO in patients with abnormal perfusion ($74.8 \pm 16.7\%$ vs 85.0 ± 8.1).

Conclusion Delayed follow-up showed CT features of acute and chronic PE but also two types of perfusion abnormalities suggestive of persistent hypercoagulability as well as unresolved/sequelae of microangiopathy.

Clinical relevance statement Despite dramatic resolution of lung abnormalities seen during the acute phase of the disease, acute pulmonary embolism and alterations at the level of lung microcirculation can be identified in patients remaining symptomatic in the year following COVID-19.

Key Points

- *This study demonstrates newly developed proximal acute PE/thrombosis in the year following SARS-CoV-2 pneumonia.*
- *Dual-energy CT lung perfusion identified perfusion defects and areas of increased iodine uptake abnormalities, suggestive of unresolved damage to lung microcirculation.*
- *This study suggests a complementarity between HRCT and spectral imaging for proper understanding of post COVID-19 lung sequelae.*

Keywords CT angiography · Respiratory system abnormalities · COVID-19 · Perfusion

✉ Martine Remy-Jardin
martine.remy@chu-lille.fr

[1] Department of Thoracic Imaging, ULR 2694 METRICS Evaluation des technologies de Santé et des pratiques médicales, Univ. Lille, CHU Lille, F-59000 Lille, France

[2] Department of Pulmonary Function Testing, ULR 4483, IMPECS, Univ. Lille, CHU Lille, F-59000 Lille, France

[3] Department of Biostatistics, ULR 2694 METRICS Evaluation des technologies de santé et des pratiques médicales, Univ. Lille, CHU Lille, F-59000 Lille, France

[4] Department of Pulmonology, CNRS, INSERM, Institut Pasteur de Lille, U1019, UMR 9017, Center for Infection and Immunity of Lille (CIIL), Univ. Lille, CHU Lille, F-59000 Lille, France

[5] Department of Thoracic Imaging, Heart & Lung Institute, University Hospital Center of Lille, Blvd Jules Leclercq, F-59000 Lille, France

Abbreviations

DECT	Dual-energy CT
DLCO	Diffusing capacity of the lung for carbon monoxide
FEV1	Forced expiratory volume in 1 s
FRC	Forced residual capacity
FVC	Forced vital capacity
HRCT	High-resolution CT
PFT	Pulmonary function tests
RV	Residual volume
TLC	Total lung capacity
VA	Alveolar capillary blood volume
VC	Vital capacity

Introduction

While the full range of long-term health consequences of COVID-19 is largely unclear, an important proportion of patients recovering from hospitalization complain of symptoms after discharge. The term "post-acute COVID-19 syndrome" (PACS) was proposed to define symptoms and abnormalities persisting or present beyond 12 weeks of the onset of acute COVID-19 and not attributable to alternative diagnoses [1, 2]. In a recent systematic review of 57 studies with 250,351 survivors of COVID-19, Groff et al reported that more than half of COVID-19 survivors still experienced PACS 6 months after recovery, the most common PACS involving functional mobility impairments, pulmonary abnormalities, and mental health disorders [3].

When persisting respiratory symptoms are in the front line, their management requires differentiation of true respiratory complications from deconditioning or depression commonly reported even 6 months after symptom onset [4]. When persistent symptoms are likely to represent sequelae of SARS-CoV-2 pneumonia, it remains to be understood the underlying mechanisms that currently rely on our knowledge of the pathophysiology of this viral infection and temporal changes in imaging findings. Over weeks, COVID-19 pulmonary findings resolve or can evolve into a more structured and organized phase, in which GGOs and consolidation transform into more reticular opacities and fibrosis-like abnormalities. Despite the dramatic improvement of lung abnormalities usually observed on radiographic and/or CT examinations, the prevalence of respiratory symptoms may remain high and stable up to 6 months after discharge [5].

In this context, sequelae of the SARS-CoV-2 infection at the level of the pulmonary circulation should also retain attention, keeping in mind the vasculocentric nature of disease currently emphasized [6–8]. During acute infection, early autopsy studies reported severe endothelial injury, capillary thrombi, and extensive new vessel growth predominantly occurring through a mechanism of intussusceptive angiogenesis [9–11]. More proximally, CT angiography depicted acute pulmonary artery embolism (PE)/thrombosis in 14.7 to 17% of hospitalized patients [12–14] while proximal pulmonary venous obstruction was only described in a single patient [15]. An in vivo insight into distal pulmonary angiopathy was reported when dual-energy CT (DECT) angiography was obtained during hospitalization, describing perfusion abnormalities within areas of consolidation as well as perfusion defects in normal-appearing lung parenchyma even in the absence of visible pulmonary artery thrombosis [16–21].

In the context of PACS, temporal changes at the level of proximal and distal pulmonary circulation have only been investigated in two studies [22, 23]. Both obtained in the early follow-up after infection, these studies reported newly developed proximal acute PE/thrombosis and DECT perfusion abnormalities, suggestive of persistent hypercoagulability as well as unresolved damage to the lung microcirculation. The goal of the present study was to evaluate COVID-19-related abnormalities at the level of the pulmonary circulation in patients remaining symptomatic in the year following hospitalization for SARS-CoV-2 pneumonia.

Materials and methods

Study population

This retrospective, non-interventional observational study was approved by the local Ethics Committee under number HP 22/07 with waiver of patient informed consent in agreement with national regulations. The study population of 79 patients was selected following the successive steps summarized in Supplementary Fig. 1 and further detailed in Supplementary Material 1.

Imaging evaluation

CT protocol

CT examinations were obtained on a 3rd-generation dual-source CT system (Somatom Definition Force; Siemens Healthineers) (Supplementary Material 2). They included standard morphologic and perfusion images, the latter generated by subtraction of low- and high-monoenergetic images (eXamine prototype; Siemens Healthineers). The percentage of COVID-19 lung infiltration, further referred to as the CT COVID score, was calculated using an AI-software prototype (CT Pneumonia Analysis; Siemens Healthineers). The software outputs a percentage of total lung involvement (by both GGO and consolidation) [24]. The CT COVID score at the time of acute pneumonia could be retrospectively calculated in 64 patients. Follow-up chest CTA was systematically

completed by a volumetric, non-contrast, single-energy acquisition at expiration to detect air trapping, i.e., a potential confounder for perfusion defect interpretation.

Analysis of CT images

Analysis of mediastinal and perfusion images On mediastinal images, we searched for the presence of endoluminal filling defects from central to subsegmental pulmonary arterial divisions. In the context of COVID-19, recent/acute obstruction of pulmonary arteries is more considered a phenomenon of in situ thrombosis rather than resulting from a thromboembolic event; these features will thus be described as acute PE/thrombosis throughout the manuscript.

On perfusion images, we rated the presence of (a) 3 types of perfusion defects (i.e., patchy defects; PE-type defects, and non-systematized areas of hypoperfusion); and (b) areas of increased perfusion. Using a prototype software (eXamine; Siemens Healthineers), we calculated the iodine concentration on perfusion images, expressed in mg of iodine/mL of lung volume. This index was obtained for both lungs, as established by the software; it did not rely on measurements of regions-of-interest. It was also retrospectively calculated for the 64 patients of our cohort in whom chest CT had also been obtained at the time of acute pneumonia.

Analysis of lung images We recorded the presence of post COVID-19 abnormalities, including ground-glass opacities (GGO); fine linear, reticular opacities; parenchymal distortion, irregular interfaces; band-like opacities; consolidation; honeycombing; and cysts, bronchial, and/or bronchiolar dilatation further referred to as bronchomegaly. At a patient level, these findings led us to consider 3 patterns of post COVID-19 abnormalities: (a) unequivocal signs of fibrosis (i.e., volume loss, marked traction bronchiectasis/bronchiolectasis, and/or honeycombing); (b) fibrotic-like abnormalities (i.e., fine linear, reticular opacities; bronchomegaly; irregular interfaces and/or parenchymal distortion; cysts); and (c) non-fibrotic abnormalities (i.e., isolated GGOs and/or band-like opacities). We also searched for the presence of vascular tree-in-bud pattern and abnormally dilated peripheral vessels [16]. Emphysema was rated as mild when limited to centrilobular emphysema, moderate when lung destruction was more pronounced but not reaching the level of panlobular emphysema, and severe in presence of panlobular emphysema. The extent of emphysema was rated as limited when involving exclusively the upper lobes, and diffuse when observed from top to bottom of the lungs. The presence of air trapping was assessed on expiratory images, rated as focal when present in ≤ 2 lobes and multifocal when present in ≥ 3 lobes.

Pulmonary function tests (PFTs)

They included a spirometry with forced vital capacity (FVC) and slow vital capacity (VC), plethysmographic lung volumes, and a single-breath DLCO according to ATS/ERS guidelines [25, 26]. The reference values used were those of the Official Statement of the European Respiratory Society [25, 27]. Functional profiles were defined as follows: (a) airway obstruction by a reduced FEV1/FVC below the 5th percentile of the predictive value; (b) lung restriction by a reduction of total lung capacity (TLC) below the 5th percentile of the predictive value and a normal FEV1/FVC; (c) alteration of lung diffusion capacity DLCO by a DLCO lower than the 5th percentile of the predicted value [28]. Among the 62 patients who underwent PFTs, all parameters were recorded except DLCO that could not be measured in 1 patient owing to the impossibility to maintain apnea.

Study endpoints

The primary endpoint was to evaluate the presence of endoluminal clots and abnormalities of lung microcirculation on DECT iodine maps. The secondary endpoint was to search for potential relationships between perfusion alterations and clinical, functional characteristics of the study population.

Conditions of image analysis

The reading of images was obtained by consensus between a senior (M.R.J.) and a junior (I.M.) chest radiologists with 30 and 5 years of experience, respectively. Quantitative perfusion analysis was an automated process, supervised by a CT technologist. Morphologic images were analyzed by the junior reader, several weeks after the reading of perfusion images. Following statistical analysis, a third and simultaneous reading of lung (inspiration and expiration) and perfusion images was undertaken by the two readers in all cases where PE-type perfusion defects had been detected. The goal of this specific evaluation was to exclude PE-type defects seen with the concurrent presence of CT features of small-airway disease, thus retaining isolated PE-type defects as manifestations of post COVID-19 pneumonia. This combined reading of lung and perfusion images also allowed the readers to superimpose perfusion abnormalities on the corresponding morphological background.

Statistical analysis

Categorical variables are expressed as number and percentages. Continuous variables were reported as means and standard deviations (SD) in the case of normal distribution or medians (interquartile, IQR) otherwise. Normality of distributions was assessed using histograms and the

Shapiro-Wilk test. Comparisons of clinical data and PFTs between patients with normal and abnormal perfusion were performed with the Mann-Whitney test for quantitative variables and the Fisher exact test for categorical variable. The association between the finding of defects and areas of increased perfusion and the time elapsed between the date of hospitalization for COVID-19 (categorized into quartiles) and the date of chest CT examination was tested using the chi-square test. Statistical testing was conducted at the two-tailed α-level of 0.05 and was considered an exploratory analysis. Data were analyzed using the SAS software version 9.4 (SAS Institute Inc.).

Results

Characteristics of the study population

The mean (± standard deviation) interval of time between COVID-19 and the delayed CT follow-up was 7.93 ± 1.7 months (median (Q1, Q3): 7.7 (6.4; 8.8); range: 5.8–11.5). As shown in Table 1, the study population included 57 males and 22 females with a mean age of 63.2 years; there were 38 smokers (48.1%). The mean values of functional parameters were within normal range; 13 patients (21%) had a restrictive pattern and 4 patients (6.4%) an obstructive pattern. DLCO-predicted values were normal in 31 patients (50.8%) and decreased in 30 patients (49.2%). The clinical and biological data of the study population at the time of COVID-19 lung infection are summarized in Supplementary Material 3.

Lung parenchymal findings

Post COVID-19 residual findings were identified in 67 patients (85%) (Table 2) while 12 patients (15%) had a complete resolution of lung abnormalities. The median CT COVID score at the time of delayed CT follow-up was 1.09% (0.33; 3.93). In the 64 patients with chest CT also obtained at the time of acute pneumonia, the median CT COVID score decreased from 45.4% (61.4; 93.9) to 1.18% (3.9; 0.3). Emphysema was found in 16 patients, rated as severe ($n = 2$), moderate ($n = 6$), and mild ($n = 8$), with a diffuse ($n = 2$) or limited ($n = 14$) extent. A vascular tree-in-bud pattern was identified in 5 patients (6.3%); abnormally dilated peripheral vessels were not seen. Air trapping was identified in 33 patients (41%), rated as focal in 13 patients (16%) and multifocal in 20 patients (25%); 22 of the 33 patients with air trapping were smokers.

Table 1 Characteristics of the study population at the time of delayed CT follow-up

	Results
Clinical variables ($n = 79$)	
Males, *n* (%)/females, *n* (%)	57 (72.1%)–22 (27.9%)
Age, year	
Mean ± SD	63.2 ± 10.2
Range	34–86
Smokers, *n* (%)	38 (48.1%)
Tobacco consumption, pack year	
Median (Q1; Q3)	20.0 (14.0; 30.0)
Range	1–41
Respiratory co-morbidities, *n* (%)	
-Emphysema, *n*	16 (20.2%)
-Asthma, *n*	8 (10.1%)
-Interstitial lung disease, *n*	0
-Peripheral lung carcinoma, *n*	0
Patient medical history, *n* (%)	
-Chronic kidney disease, *n*	6 (7.6%)
-Cardiovascular disease, *n*	10 (12.7%)
-Type 2 diabetes, *n*	14 (17.7%)
-Hypertension, *n*	30 (38%)
-Extra-thoracic tumor, *n*	0
Body mass index (BMI), kg/m^2	
Mean ± SD	33.6 ± 6.1
Range	20–50
Body mass index (BMI) categories	
-< 18.5 kg/m^2 *(underweight patient)*, *n* (%)	0
-18.5– < 25 kg/m^2 *(normal BMI)*, *n* (%)	1 (1.3%)
-25–30 kg/m^2 *(overweight patient)*, *n* (%)	23 (29.1%)
-> 30 kg/m^2 *(obese patient)*, *n* (%)	55 (69.7%)
Functional parameters ($n = 62$)	
VC, %pred	
Mean ± SD	98.2 ± 18.7
Range	52.9–152
FVC, %pred	
Mean ± SD	97.9 ± 19.9
Range	52.3–149
FEV1/FVC	
Mean ± SD	80.1 ± 8.5
Range	43.2–94.9
FRC, %pred	
Mean ± SD	87.0 ± 17.0
Range	46.3–143
RV, %pred	
Mean ± SD	86.1 ± 19.6
Range	50.9–148
TLC, %pred	
Mean ± SD	90.7 ± 12.9
Range	64–117

Table 1 (continued)

	Results
DLCO, %pred	
Mean ± SD	76.0 ± 16.3 *(1 missing)*
Range	39–116
DLCO/VA, %pred	
Mean ± SD	96.6 ± 16.1
Range	62–126
Functional profiles ($n = 62$)	
-Normal PFTs, *n* (%)	45/62 (72.6%)
-Lung restriction, *n* (%)	13/62 (21%)
-Airway obstruction, *n* (%)	4/62 (6.4%)
-Decreased DLCO, *n* (%)	30/61 (49.2%) *(1 missing)*

Abbreviations: *SD*, standard deviation; *Q1*, lower interquartile; *Q3*, upper interquartile; *VC*, vital capacity; *FVC*, forced vital capacity; *FEV1*, forced expiratory volume in 1 s; *FRC*, forced residual capacity; *RV*, residual volume; *TLC*, total lung capacity; *DLCO*, diffusing capacity of the lung for carbon monoxide; *VA*, alveolar capillary blood volume

CT angiographic findings (Table 3)

CT features of isolated subsegmental and/or segmental acute PE/thrombosis were identified in 2 patients (2.5%) presenting minimal GGO in the upper lobes (1/2) or marked fibrotic-like abnormalities in both lungs (1/2). Following CT angiography, Doppler ultrasonographic examination was obtained from both patients; none had features of deep venous thrombosis. At the time of acute viral infection, none of them was diagnosed with acute PE/thrombosis; they had received preventive anticoagulation during hospitalization.

In 4 patients, there were CT features of chronic obstruction of PAs, considered (a) sequelae of acute PE/thrombosis (*diagnosed during the acute phase of the viral pneumonia and treated by anticoagulation*) in 3 patients (4%), based on the comparison of CT findings at the time of COVID-19 hospitalization and follow-up; and (b) sequelae of a previous episode of acute PE, documented 3 years prior to COVID-19, thus unrelated to COVID-19 in 1 patient. The 3 patients with post COVID-19 chronic clots had isolated subsegmental and/or segmental chronic PE. Doppler ultrasonographic examination was not obtained at the time of CT follow-up. CT angiographic images of the 18 patients excluded from the study population because of non-interpretable perfusion images were analyzed; none showed features of acute and/or chronic PE.

Lung perfusion findings (Table 4)

The interobserver agreement for the reading of perfusion images was 0.81 [95%CI: 0.62–0.99]. Perfusion was rated as normal in 10 patients (12.6%) and abnormal in 69 patients (87.4%) among whom there were 4 patients with complete resolution of COVID-19 lung infiltration and no emphysema on lung images.

Perfusion abnormalities consisted of a variable association of (a) patchy perfusion defects (60/79; 76%), always bilateral (Fig. 1); (b) focal areas of non-systematized hypoperfusion (27/79; 34.2%), seen as unilateral (7/27) or bilateral (20/27) findings; and (c) PE-type perfusion defects (14/79; 17.7%) seen as unilateral (10/14) or bilateral (4/14) findings. PE-type defects were seen in the anatomical zones of acute PE/thrombosis (2/14) and

Table 2 Residual COVID-19 lung abnormalities at the time of delayed CT follow-up

CT features ($n = 79$)	
Inspiratory CT scans	
Ground-glass opacities, *n* (%)	65 (82.3%)
Fine linear, reticular opacities, *n* (%)	58 (73.4%)
Band-like opacities, *n* (%)	20 (25.3%)
Bronchomegaly, *n* (%)	28 (35.4%)
Parenchymal distortion, irregular interfaces, *n* (%)	32 (40.5%)
Vascular tree-in-bud, *n* (%)	5 (6.3%)
Cysts, *n* (%)	3 (3.8%)
Abnormally dilated peripheral vessels, *n* (%)	0
Expiratory CT scans	
Air trapping, *n* (%)	33 (41%)
CT patterns	
Unequivocal signs indicative of established fibrosis, *n* (%) *(volume loss, marked traction bronchiectasis, and/or honeycombing)*	0
Fibrotic-like abnormalities, *n* (%) *(linear and/or reticular opacities; bronchomegaly; irregular interfaces; and/or parenchyma distortion; cysts)*	32 (40.5%)
Non-fibrotic abnormalities, *n* (%) *(ground-glass opacities; band-like opacities)*	35 (44.3%)

Table 3 CT angiographic findings in the study population at the time of delayed CT follow-up

CT features of acute pulmonary embolism ($n=2$)	Location of endoluminal clots	Recent lung infarction	Residual COVID-19 pneumonia	Doppler ultrasonography at the time of CT follow-up
Case 1	Subsegmental clot in RA3	No	Mild GGO in the upper lobes	Normal
Case 2	Segmental and subsegmental clots in RA10	No	Marked bilateral fibrotic-like abnormalities	Normal
CT features of chronic PE ($n=4$)	Location of chronic clots	Sequelae of lung infarction	Residual COVID-19 pneumonia	Doppler ultrasonography at the time of CT follow-up
Sequelae of acute PE diagnosed during COVID-19 pneumonia (3 patients)				
Case 1	Segmental and subsegmental clots in RA1, RA2 *At the time of COVID-19: acute PE in RA1; no venous thrombosis at Doppler ultrasonography*	No	Bilateral, mild GGO	Not performed
Case 2	Subsegmental chronic clot in RA10 *At the time of COVID-19: bilateral central and peripheral acute PE; complete mesenterico-caval thrombosis*	No	No residual abnormality	Not performed
Case 3	Subsegmental chronic clot in LA7+8 *At the time of COVID-19: bilateral central and peripheral acute PE with RV strain*	No	Mild GGO, band-like opacities	Not performed
Unrelated to COVID-19 pneumonia (one patient)				
Case 4	RA9, LA4, LA5, LA10 *Bilateral central and peripheral acute PE 4 years earlier*	No	Bilateral fibrotic-like abnormalities	Not performed

Table 4 Description of perfusion findings at the time of delayed CT follow-up of the study population ($n=79$)

		$n=79$
Overall findings	(1) Normal perfusion	10 (12.6%)
	-residual COVID-19 abnormalities on lung images	2/10
	-complete resolution of COVID-19 abnormalities on lung images	8/10
	(2) Abnormal perfusion	69 (87.4%)
	-residual COVID-19 abnormalities on lung images	65/69
	-complete resolution of COVID-19 abnormalities on lung images	4/69
Perfusion abnormalities	(1) Patchy defects, *n* (%)	60 (76%)
	(2) Focal areas of hypoperfusion, *n* (%)	27 (34.2%)
	(3) PE-type defects, *n* (%)	14 (17.7%)
	-beyond acute clots, *n*	2/14
	-beyond chronic clots, *n*	4/14
	-seen in the absence of clots, air trapping	8/14
	(4) Focal areas of increased perfusion	59 (74.9%)
	-superimposed on GGOs	58/59
	-superimposed on band-like opacities	51/59
	-superimposed on vascular tree-in-bud	5/59

focal chronic PE (4/14) (Supplementary Fig. 2) but also in the absence of endoluminal clot or air trapping (8/14) (Fig. 2). Supplementary Fig. 5 illustrates how these patterns coexisted: (a) the three patterns of perfusion defects coexisted in 6 patients (6/79; 3.8%); (b) 18 patients (18/79; 22.8%) had patchy defects and focal areas of non-systematized hypoperfusion; (c) 8 patients (8/79; 10.1%) had PE-type defects and patchy defects. In 16 patients, no perfusion defects were detected. Focal areas of increased perfusion were identified in 59 patients (74.9%), always superimposed on areas of GGO (58/59), band-like opacities (51/59), and/or areas of vascular tree-in-bud (5/59) (Figs. 3 and 4). The combinations of perfusion defects and areas of increased perfusion included (a) defects and areas of increased perfusion: $n=55$ (69.6%); (b) defects alone: $n=8$ (10.1%); and (c) areas of increased perfusion alone: $n=4$ (5.1%). In 12 patients (15.1%), there were no defects nor areas of increased perfusion.

Figures 5 and 6 illustrate the timeline of defects and the timeline of areas of increased perfusion according to the time elapsed between the date of hospitalization for COVID-19 (categorized in quartiles) and chest CT examination. The quartiles comprise the following: quartile 1: <6.4 months; quartile 2: 6.4 to 7.7 months; quartile 3: 7.7 to 8.8; quartile 4: ≥ 8.8 months. No association was found between the finding of defects and quartiles of time elapsed between the date of hospitalization for COVID-19 and chest CT examination ($p=0.86$) nor between the finding of areas of increased perfusion and the quartiles ($p=0.58$) (chi-square test).

Comparison of patients with normal and abnormal perfusion

Compared to patients with normal perfusion (Table 5), patients with abnormal perfusion had a significantly greater extent of residual post COVID-19 lung infiltration

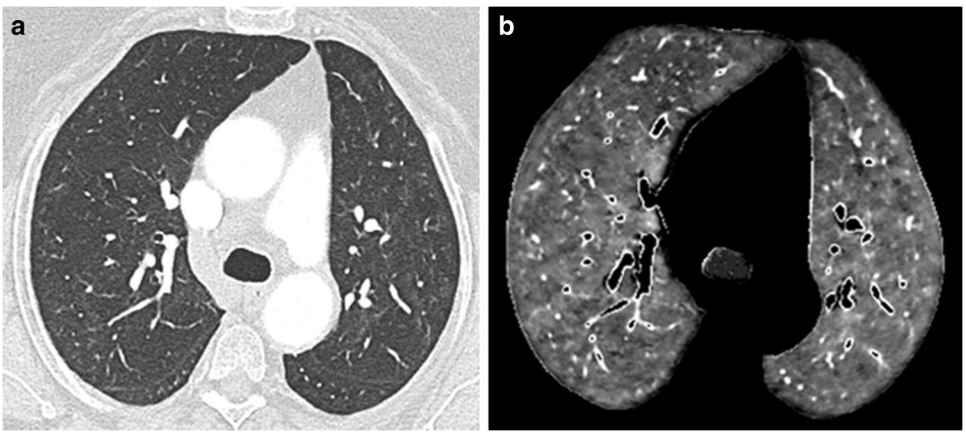

Fig. 1 Dual-energy CT angiography obtained in a 76-year-old, nonsmoker, obese female (BMI: 47.3 kg/m^2), 29 weeks after COVID-19 pneumonia that had required oxygen supplementation. Lung image (**a**) obtained at the level of the upper lobes and corresponding perfusion image (**b**). Note the presence of numerous patchy areas of hypoperfusion in the absence of morphological abnormalities in both upper lobes

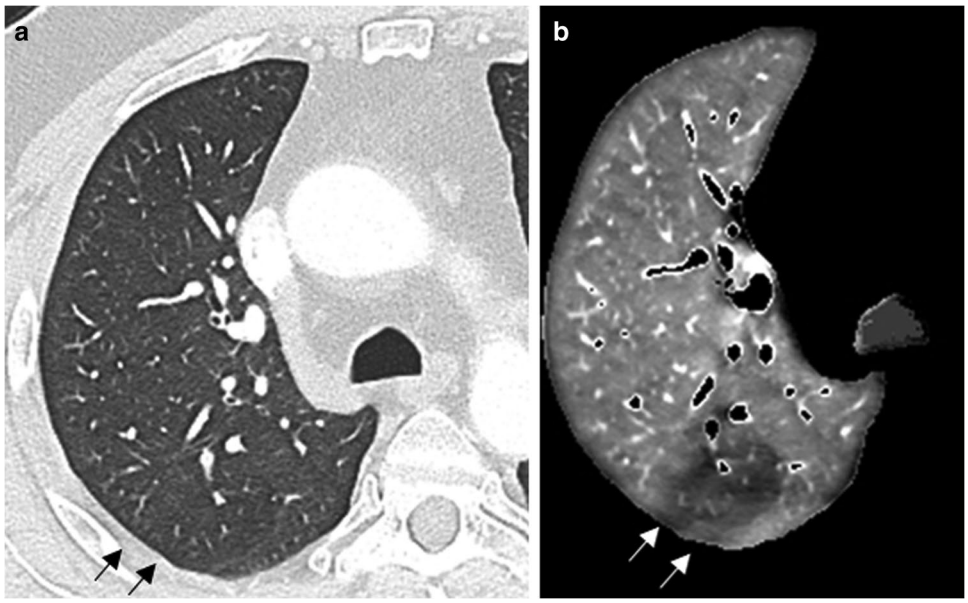

Fig. 2 Dual-energy CT angiography obtained in a 63-year-old obese male (BMI: 31.2 kg/m^2), nonsmoker, 32 weeks after COVID-19 pneumonia that had required invasive ventilation. Lung image obtained at the level of the carina (magnified view of the right upper lobe; **a**). Note the absence of lung parenchymal abnormality, especially in the posterior segment of the right upper lobe (arrows). Corresponding perfusion image (**b**) showing a peripheral PE-type defect in the posterior segment of the right upper lobe (arrows)

($p = 0.004$) but did not differ in BMI ($p = 0.92$), number of smokers ($p = 0.51$), gender (0.45), hospitalization in the ICU (0.15), or mechanical ventilation ($p = 0.44$). There was no significant difference in the presence of emphysema ($p = 0.11$) nor in the iodine concentration ($p = 0.59$). There was no statistically significant difference in the median values of PFT parameters between patients with normal and abnormal perfusion. The median value of DLCO %pred was lower in patients with abnormal perfusion compared to that in patients with normal perfusion (73.0% vs 81.0%) but this difference did not reach statistical difference ($p = 0.08$). The distribution of functional profiles did not differ; the proportion of patients with decreased DLCO %pred was greater among patients with abnormal perfusion ($n = 29$; 53%) compared with patients with normal perfusion ($n = 1$; 14%).

Discussion

To our knowledge, this is the first study providing detailed analysis of morpho-functional changes at the level of the pulmonary circulation in patients with persistent symptoms more than 6 months after recovery from COVID-19. At the time of this delayed CT follow-up, all patients had a dramatic resolution of the radiographic features of

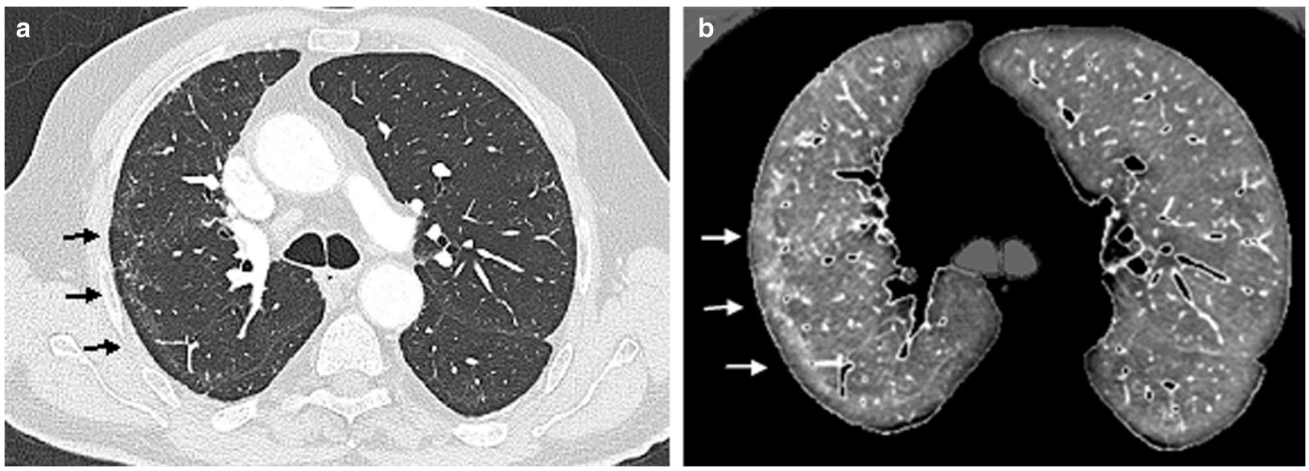

Fig. 3 Dual-energy CT angiography obtained in a 60-year-old obese male (BMI: 32.5 kg/m^2), 24 weeks after COVID-19 pneumonia that had required oxygen supplementation. Lung image obtained at the level of the upper lobes (**a**) showing the presence of post COVID-19 residual ground-glass opacities in the subpleural lung parenchyma of the right upper lobe (arrows). Corresponding lung perfusion image (**b**), showing areas of increased perfusion superimposed on ground-glass opacities (arrows)

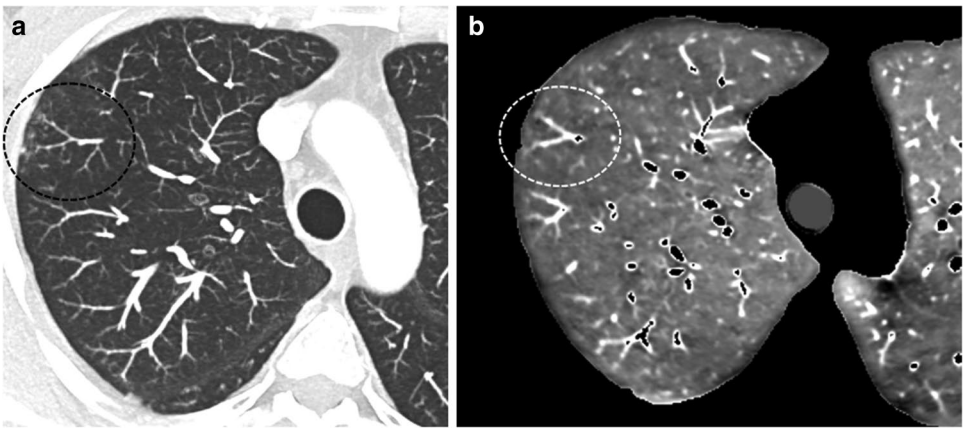

Fig. 4 Dual-energy CT angiography obtained in a 57-year-old obese male (BMI: 31.2 kg/m2), 32 weeks after COVID-19 pneumonia with oxygen requirement. **a** Lung image (magnified view; 5-mm-thick maximum intensity projection) obtained at the level of the right upper lobe showing a vascular tree-in-bud pattern (dotted circle). **b** Corresponding perfusion image showing tubular areas of increased perfusion superimposed on the vascular tree-in-bud pattern (dotted circle)

COVID-19 pneumonia with a complete clearing of lungs in 12 patients (15%) and residual findings in 67 patients (85%) with a median COVID-19 CT score decreasing from 45.4 to 1.18%. Residual findings included fibrotic-like and non-fibrotic abnormalities in 32 (40.5%) and 35 (44.3%), respectively, and none of our patients had unequivocal signs indicative of established lung fibrosis.

In this background of post COVID-19 lung parenchymal changes, we observed focal features of chronic obstruction of pulmonary arteries linked to COVID-19 in 3 patients (4%), seen in subsegmental and/or segmental pulmonary arteries of one or two segments. We also identified focal features of acute PE/thrombosis in 2 patients (2.5%), depicted in subsegmental and/or segmental arteries of a single segment. These clots were identified without peripheral venous thrombosis, reinforcing the presumption of in situ thrombosis previously highlighted during the acute phase of COVID-19 but also suggesting persistent coagulation abnormalities. Using CT angiography in the early CT follow-up of COVID-19, acute PE/thrombosis was reported in 5.4% of the studied population [23]. While awaiting for more data from long-term follow-up studies, evidence is emerging of delayed complications at the level of the pulmonary circulation [29]. A study investigating a large cohort of patients discharged from three hospitals after COVID-19 reported PE events occurring within 45 days after hospital discharge [30]. Using Swedish national registry data, the incidence rate ratio for PE remained elevated during days 91–180 after COVID-19 [31]. The risk of developing chronic thromboembolic pulmonary hypertension following COVID-19-associated acute PE is subsequently of great concern among COVID-19 survivors [32].

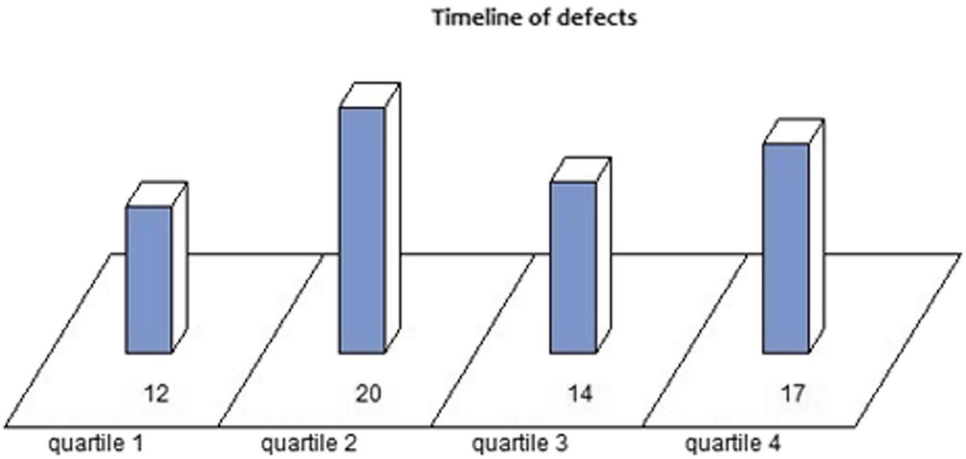

Fig. 5 Timeline of perfusion defects according to the time elapsed between the date of hospitalization for COVID-19 (categorized in quartiles) and chest CT examination (quartile 1: <6.4 months; quartile 2: 6.4 to 7.7 months; quartile 3: 7.7 to 8.8; quartile 4: ≥8.8 months). No association was found between the finding of perfusion defects and the quartiles ($p=0.86$) (chi-square test). This diagram illustrates the various combinations of perfusion defects observed in the study population. The three patterns of perfusion defects coexisted in 6 patients (6/79; 3.8%); 18 patients (18/79; 22.8%) had patchy defects and focal areas of non-systematized hypoperfusion; 8 patients 8/79; 10.1%) had PE-type defects and patchy defects. In 16 patients, no perfusion defects were detected

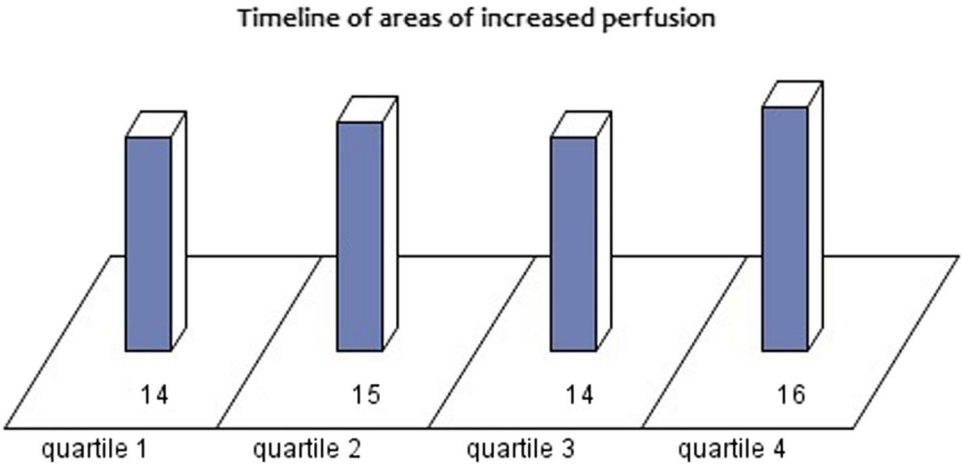

Fig. 6 Timeline of areas of increased perfusion according to the time elapsed between the date of hospitalization for COVID-19 (categorized in quartiles) and chest CT examination (quartile 1: < 6.4 months; quartile 2: 6.4 to 7.7 months; quartile 3: 7.7 to 8.8; quartile 4: ≥ 8.8 months). No association was found between the finding of areas of increased perfusion and the quartiles ($p = 0.58$) (chi-square test)

The reading of perfusion images depicted perfusion abnormalities in 69 patients (87.4%). Two types of alterations were observed, namely perfusion defects and areas of increased perfusion. As previously reported in the early DECT follow-up of COVID-19, the presence of disseminated patchy perfusion defects was the most frequent finding, seen in 60 (76%) patients. PE-type defects were seen in 14 patients (17.7%), logically depicted beyond acute and chronic obstruction of pulmonary arteries in 6 patients. However, small-sized, peripheral PE-type defects were seen in 8 patients in whom there were no features of endoluminal clots or small-airway disease, the latter being a well-known cause of PE-type perfusion defects. It is interesting to note that the three patterns of perfusion defects coexisted in 6 patients (3.8%) while the most frequent associations combined two patterns, namely patchy defects and focal areas of non-systematized hypoperfusion, seen in 18 patients (22.8%), and patchy defects and PE-type defects seen in 8 patients (10.1%). In the absence of pathologic CT correlations, a relationship between patchy defects and unresolved

Table 5 Comparison of clinical and CT characteristics between patients with normal and abnormal perfusion in the study population ($n = 79$)

	Patients with normal perfusion $n = 10$	Patients with abnormal perfusion $n = 69$	p value
Gender (males/females), *n*	6/4	51/18	0.45
Age, year			0.11
Median (Q1–Q3)	58.5 (55.0; 63.0)	64.0 (57.0; 69.0)	
Range	37.0–73.0	34.0–86.0	
BMI, kg/m^2			0.92
Median (Q1–Q3)	31.8 (28.7–71.6)	32.6 (28.9–37.0)	
Range	27.2–45.6	20.9–50.1	
Smokers, *n* (%)	6 (60%)	32 (46.4%)	0.51
Hospitalization in the ICU, *n* (%)	5 (50%)	24 (74%)	0.15
Mechanical ventilation, *n* (%)	1 (10%)	19 (27.5%)	0.44
Residual COVID-19 lung infiltration			**0.004**
Median (Q1–Q3)	0.2 (0.03; 0.59)	1.26 (0.5; 6.80)	
Range	0–2.9	(40–45.1)	
Emphysema, *n* (%)	4 (40%)	12 (17.4%)	0.11
Iodine concentration, mg/mL			0.59
Median (Q1–Q3)	1.18 (0.85; 1.70)	1.14 (0.85–1.34)	
Range	0.5–2.03	0.26–2.66	

Abbreviations: *Q1*, lower interquartile; *Q3*, upper interquartile; *ICU*, intensive care unit; *BMI*, body mass index

NB: Comparisons were obtained with the Fisher exact test for qualitative variables and the Mann–Whitney test for quantitative variables

microthrombi at the level of pulmonary capillaries can be raised while PE-type defects could be considered sequelae of thrombi within pulmonary arteries with a diameter of 1 to 2 mm developed during acute pneumonia, often seen with venous thrombosis [8].

The second intriguing finding was the presence of focal areas of increased perfusion in 59 patients (74.9%), always superimposed on residual COVID-19 abnormalities, such as GGOs and/or band-like opacities, and tubular areas of increased perfusion superimposed on vascular tree-in-bud abnormalities in 5 patients. In the absence of pathologic CT correlations, one can suggest the possibility of persistent aberrant angiogenesis taking place at the capillary level that was described during the acute phase of COVID-19 pneumonia [9], as well as dilated intrapulmonary bronchopulmonary anastomoses more recently highlighted [33, 34]. However, our attention was drawn by a recent study from Ravaglia et al who reported pathologic clues in 10 patients with persistent lung disease who underwent lung cryobiopsies on average 3.5 months after recovery [35]. These authors described a cluster characterized by diffuse vascular increase with dilatation of the lumen of alveolar capillaries and venules and hyperplasia of capillaries within an otherwise normal or minimally abnormal parenchyma, similar in some aspects to pulmonary capillary hemangiomatosis. Compared to DECT findings in the 3 months following COVID-19, we observed similar proportions of patchy defects (76% vs 83% at 3 months) and PE-type defects (17.7% vs 16.6% at 3 months) but a higher proportion of focal areas of increased perfusion (74.9% vs 41.6%) [23].

Regarding PFTs, they were normal in 72.6% of the study population. When abnormal, the most frequent profile was a restrictive pattern, seen in 21% of our study group. This ventilatory disorder is a common finding in the early follow-up of COVID-19 [36, 37] and impaired TLC has also been reported in 14% of patients at 6 months [38]. In the current view of the vasculocentric nature of the disease [6, 7], it is worth noting that 49.2% of our cohort had decreased DLCO, previously reported in 16 to 54% of patients at 3 months [39, 40] and in 37.2% and 32.1% of patients at 6 months [38, 41].Whereas the median values of functional parameters and ventilatory profiles did not differ between patients with normal and abnormal perfusion, we observed that 53% of patients with abnormal perfusion had a decrease in DLCO versus 14% of the patients with normal perfusion. This was seen in the absence of significant difference in the proportion of smokers between the two groups, emphasizing the likelihood of persistent alterations at the level of lung microcirculation in a cohort without unequivocal signs of established fibrosis. Quantification of iodine within both lungs did not show significant differences between the subgroups analyzed, probably explained by subtle perfusion alterations and compensatory effects between defects and areas of hyperperfusion.

Several limitations of this study have to be acknowledged. First, we evaluated a relatively small number of participants, all of whom were symptomatic; therefore, we cannot comment on the prevalence of pulmonary function testing and imaging abnormalities among all survivors of COVID-19. However, this cohort enabled us to describe in detail DECT lung perfusion changes, not previously reported in the literature. Second, we gathered patients from 3 periods of the pandemic with differences in treatment during acute viral infection since the onset of the disease but also with differences in the viral variants responsible for lung pneumonia. However, all patients were offered a similar post COVID-19 management ensuring homogeneous evaluation of residual CT findings. Third, we did not include serial imaging which might have been interesting owing to the similarity of changes seen during the early and delayed CT follow-up. This was dictated by the limited number of patients who were scanned twice after the initial infection that would have limited the description of longitudinal changes to 35 patients scanned between 2.7 and 4.8 months after COVID-19. Last, there was no control group, explained by the fact that there is no generalized follow-up of viral pneumonia.

In conclusion, this study shows a striking difference between the limited extent of CT features of COVID-19 pneumonia and the presence of numerous abnormalities at the level of lung microcirculation in the year following hospitalization. Our results suggest the complementarity between HRCT and spectral imaging for proper understanding of post COVID-19 lung sequelae.

Supplementary Information The online version contains supplementary material available at https://doi.org/10.1007/s00330-023-09618-9.

Funding The authors state that this work has not received any funding.

Declarations

Guarantor The scientific guarantor of this publication is Martine Remy-Jardin.

Conflict of interest A software prototype enabling quantification of the iodine concentration in lung anatomical regions was developed by Siemens Healthineers. The authors of this manuscript declare no other relationships with any companies whose products or services may be related to the subject matter of the article.

Statistics and biometry Pr Alain Duhamel kindly provided statistical advice for this manuscript.

Informed consent Written informed consent was waived by the Institutional Review Board.

Ethical approval Institutional Review Board approval was obtained.

Methodology
- retrospective
- observational
- performed at one institution

References

1. Nalbandian A, Sehgal K, Gupta A et al (2021) Post-acute COVID-19 syndrome. Nat Med 27:601–615
2. (2020) COVID-19 rapid guideline: managing the long-term effects of COVID-19. London, National Institute for Health and Care Excellence (UK). Available from www.ncbi.nih.gov/books/NBK567261/. Accessed June 2022
3. Groff D, Sun A, Ssentongo AE et al (2021) Short-term and long-term rates of postacute sequelae of SARS-CoV-2 infection: a systematic review. JAMA Netw Open 4:e2128568
4. Huang L, Yao Q, Gu X et al (2021) 1-year outcomes in hospital survivors with COVID-19: a longitudinal cohort study. Lancet 398:747–758
5. Darcis G, Bouquegneau A, Maes N et al (2021) Long-term clinical follow-up of patients suffering from moderate-to-severe COVID-19 infection: a monocentric prospective observational cohort study. Int J Infect Dis 109:209–216
6. George PM, Desai SR (2021) COVID-19 pneumonia and the pulmonary vasculature: a marriage in hell. Eur Respir J 58:2100811
7. Oudkerk M, Kuijpers D, Oudkerk SF, Van Beek EJR (2020) The vascular nature of COVID-19. Br J Radiol 93:20200718
8. McGonagle D, Bridgewood C, Ramanan AV et al (2021) COVID-19 vasculitis and novel vasculitis mimics. Lancet Rheumatol 3:e224–e233
9. Ackerman M, Verleden SE, Kuehnel M et al (2020) Pulmonary vascular endothelialitis, thrombosis and angiogenesis in COVID-19. N Engl J Med 383:120–128
10. Varga Z, Flammer AJ, Steiger P et al (2020) Endothelial cell infection and endotheliitis in COVID-19. Lancet 395(10234):1417–1418
11. Fox SE, Akmatbekov A, Harbert JL et al (2020) Pulmonary and cardiac pathology in African American patients with COVID-19: an autopsy series from New Orleans. Lancet Respir Med 8:681–686
12. Jimenez D, Garcia-Sanchez A, Rali P et al (2021) Incidence of VTE and bleeding among hospitalized patients with coronavirus disease in 2019. Chest 159:1182–1196
13. Suh YJ, Hong H, Ohana M et al (2021) Pulmonary embolism and deep vein thrombosis in COVID-19: a systematic review and meta-analysis. Radiology 298: E70-E80
14. Tan BK, Mainbourg S, Friggeri A et al (2021) Arterial and venous thromboembolism in COVID-19: a study-level meta-analysis. Thorax 76:970–979
15. Goddard S, Tran DQ, Chan MF et al (2021) Pulmonary vein thrombosis in COVID-19. Chest 159:e361–e364
16. Patel BV, Arachchillage DJ, Ridge CA et al (2020) Pulmonary angiopathy in severe COVID-19: physiologic, imaging and hematologic observations. Am J Respir Crit Care Med 202:690–699
17. Santamarina MG, Riscal DB, Beddings I et al (2020) COVID-19: what iodine maps from perfusion CT can reveal – a prospective cohort study. Crit Care 24:619
18. Idilman IS, Dizman GT, Duzgun SA et al (2021) Lung and kidney perfusion deficits diagnosed with dual-energy computed-tomography in patients with COVID-19-related systemic microangiopathy. Eur Radiol 31:1090–1099
19. Grillet F, Busse-Coté A, Calame P et al (2020) COVID-19 pneumonia: microvascular disease revealed on pulmonary dual-energy computed tomography angiography. Quant Imaging Med Surg 10:1852–1862
20. Aydin S, Kantarci M, Karavas E et al (2021) Lung perfusion changes in COVID-19 pneumonia: a dual energy computerized tomography study. Br J Radiol 94:20201380
21. Le Berre A, Boeken T, Caramella C et al (2021) Dual-energy CT angiography reveals high prevalence of perfusion defects unrelated to pulmonary embolism in COVID-19 lesions. Insights Imaging 12:2432
22. Patelli G, Paganoni S, Besena F et al (2020) Preliminary detection of lung hypoperfusion in discharged COVID-19 patients during recovery. Eur Respir J 129:109121
23. Remy-Jardin M, Duthoit L, Perez T et al (2021) Assessment of pulmonary arterial circulation 3 months after hospitalization for SARS-CoV-2 pneumonia: dual-energy CT (DECT) angiographic study in 55 patients. EClinicalMedicine 34:100778
24. Gierarts C, Dangis A, Janssen L et al (2022) Prognostic value and reproducibility of AI-assisted analysis of lung involvement in COVID-19 on low-dose submillisievert chest CT: sample size implications for clinical trials. Radiol Cardiothorac Imaging 2:e200441
25. Wanger J, Clausen JL, Coates A et al (2005) Standardisation of the measurement of lung volumes. Eur Respir J 26(3):511–522
26. Miller MR, Hankinson J, Brusasco V et al (2005) Standardisation of spirometry. Eur Respir J 26(2):319 38
27. Macintyre N, Crapo RO, Viegi G et al (2005) Standardisation of the single-breath determination of carbon monoxide uptake in the lung. Eur Respir J 26:720–735
28. Pellegrino R, Viegi G, Brusasco V et al (2005) Interpretative strategies for lung function tests. Eur Respir J 26:948–968
29. Overton PM, Toshner M, Mulligan C et al (2022). Pulmonary thromboembolic events in COVID-19 – a systematic literature review. Pulm Circ 5:e12113. https://doi.org/10.1002/pul2.12113
30. Rashidi F, Barco S, Kamangar F et al (2021) Incidence of symptomatic venous thromboembolism following hospitalization for coronavirus disease 2019: prospective results from a multi-center study. Thromb Res 198:135–138
31. Katsoularis I, Fonseca-Rodriguez O, Farrington P et al (2022) Risks of deep vein thrombosis, pulmonary embolism, and bleeding after COVID-19: nationwide self-controlled case series and matched cohort study. BMJ 2022(377):e069590
32. Cueto-Robledo G, Roldan-Valadez E, Graniel-Palafox LE et al (2022) Chronic thrombo-embolic pulmonary hypertension (CTEPH): a review of another sequel of severe post-COVID-19 pneumonia. Curr Probl Cardiol 101187. https://doi.org/10.1016/j.cpcardiol.2022.101187
33. Ackermann M, Tafforeau P, Wagner WL et al (2022) The bronchial circulation in COVID-19 pneumonia. Am J Respir Crit Care Med 205:121–125
34. Galambos C, Bush D, Abman SH (2021) Intrapulmonary bronchopulmonary anastomoses in COVID-19 respiratory failure. Eur Respir J 58:2004397
35. Ravaglia C, Doglioni C, Chilosi M et al (2022) Clinical, radiological and pathological findings in patients with persistent lung disease following SARS-CoV-2 infection. Eur Respir J 2102411. https://doi.org/10.1183/13993003.02411-2021

36. Mo X, Jian W, Su Z et al (2020) Abnormal pulmonary function in COVID-19 patients at the time of hospital discharge. Eur Respir J 55:2001217
37. Frija-Masson J, Bancal C, Plantier L et al (2021) Alteration of diffusion capacity after SARS-CoV-2 infection: a pathophysiological approach. Front Physiol 12:624062
38. Fortini A, Torrigiani A, Sbaragli S et al (2021) COVID-19: Persistence of symptoms and lung alterations after 3–6 months from hospital discharge. Infection 49:1007–1015
39. Zhao YM, Shang YM, Song WB et al (2020) Follow-up study of the pulmonary function and related physiological characteristics of COVID-19 survivors three months after recovery. EClinicalMedicine 25:100463
40. Balbi M, Conti C, Imeri G et al (2021) Post-discharge chest CT findings and pulmonary function tests in severe COVID-19 patients. Eur J Radiol 138:109676
41. Wu Q, Zhong L, Li H et al (2021) A follow-up study of lung function and chest computed tomography at 6 months after discharge in patients with coronavirus disease in 2019. Can Respir J 2021:6692409. https://doi.org/10.1155/2021/6692409. eCollection 2021